Korean J. Chem. Eng., 35(1), 195-203 (2018)
DOI: 10.1007/s11814-017-0253-4

pISSN: 0256-1115
eISSN: 1975-7220

Zeaxanthin production by *Paracoccus zeaxanthinifaciens* ATCC 21588 in a lab-scale bubble column reactor: Artificial intelligence modelling for determination of optimal operational parameters and energy requirements

Chetan Joshi† and Rekha Satishchandra Singhal

Food Engineering & Technology Department, Institute of Chemical Technology, Matunga, Mumbai 400 019, India
(*Received 5 June 2017 • accepted 18 September 2017*)

Abstract−The operational optimization of zeaxanthin production by *Paracoccus zeaxanthinifaciens* ATCC 21588 in a bubble column reactor was performed by coupling genetic algorithm (GA) to an artificial neural network (ANN) model developed using experimental one-variable-at-a-time (OVAT) results. The effects of varying air flow rate (2-5 vvm) and inoculum size (4 and 8%) for different incubation time (30-80 h) were evaluated. Volumetric power input (P/V_L) and energy input (E) to the bubble column were then correlated with the ANN-GA optimized conditions. A maximum zeaxanthin production of 13.76±0.14 mg/L was observed at 4 vvm using an inoculum size of 4% (v/v) after 60 h of incubation in OVAT experiments with corresponding P/V_L value of 231.57 W/m^3 reflecting an energy consumption of 50.02 kJ during the fermentation period. The ANN based GA optimization predicted a maximum zeaxanthin production of 14.79 mg/L at 3.507 vvm, 4% inoculum size and 55.83 h against the experimental production of 15.09±0.51 mg/L corresponding to a P/V_L value of 202.03 W/m^3 reflecting to a significantly reduced energy input (40.01 kJ). The proposed OVAT based ANN-GA optimization approach can be used to simulate similar studies involving microbial fermentation in bioreactors.

Keywords: Artificial Neural Network, Genetic Algorithm, Zeaxanthin, Bubble Column Reactor, Fermentation

INTRODUCTION

Zeaxanthin is an odorless, orange-red, lipophilic oxycarotenoid having no provitamin A activity. It is known to function as an antioxidant and a blue light filter, and has a preventive effect on diseases like cancer [1] and age-related macular degeneration [2-4]. Industrial applications of zeaxanthin include cosmetics, poultry and pharmaceuticals [5,6]. Common food sources of zeaxanthin are corn, eggs, spinach and other yellow vegetables (and fruits). Chemically, it is synthesized by Wittig reaction. However, due to recently renewed public interest in natural pigments, exploration of microbial biosynthesis of zeaxanthin has again gained momentum [7].

Although many microbes produce zeaxanthin, only a few produce it as their major carotenoid. *Paracoccus zeaxanthinifaciens* ATCC 21588 is an aerobic bacteria that produces zeaxanthin as essentially its only carotenoid [8,9]. Aerobic microorganisms utilize oxygen for their growth, maintenance and metabolite production. Optimum oxygen transfer from air to the fermentation broth is thus veritable in bioreactor designing and operation. Among various kinds of bioreactor configurations, the bubble column is one of the simplest and most promising apparatuses for enhancing mass transfer performances in bioprocesses [10]. It consists of a cylindrical column with a high aspect ratio (H/D≥2) filled with the fermentation medium, and the air is introduced at the bottom using a sparger. The introduction of air from the bottom is solely responsible for achieving both aeration and mixing. Unlike mechanically agitated tank reactors, no mechanical stirring is provided; thus they offer numerous advantages over stirred tank vessels, such as lower maintenance and operating cost, satisfactory heat and mass transfer performance, lower shear stress and ease of process control [10-13]. Moreover, the bubble column reactor when operated at higher air flow rates has been reported to enhance the production of carotenoids due to increased oxidative stress conferred on the microorganism being cultured [11]. In bubble column reactor operations, air flow rate, inoculum size and incubation time play a vital role in determining viability of the bioprocess. Air flow rate and incubation time reflect on the energy requirements of the process, while inoculum size plays an important role in designing of the seed vessels and thus determining process economics [13].

Different traditional optimization techniques, such as one variable-at-a-time approach, response surface designs and evolutionary operations, have been extensively used to predict the optimum combination of input parameters in different bioprocesses [14-17]. In recent years, however, the artificial neural network assisted genetic algorithm (ANN-GA) technique has attracted a great deal of attention for being a superior tool for predictive modeling and optimization of complex multivariable systems [18,19]. The ANN-GA approach is particularly advantageous compared to other traditional mathematical techniques as a limited number of experiments are sufficient to empirically model and optimize a complex process with excellent accuracy without any prior knowledge of the model structure. ANN-GA technique has been applied with excellent accuracy for the predictive modeling of various chemical and biological processes such as fermentation [20-22], wastewater treat-

†To whom correspondence should be addressed.
E-mail: chetanudct@gmail.com

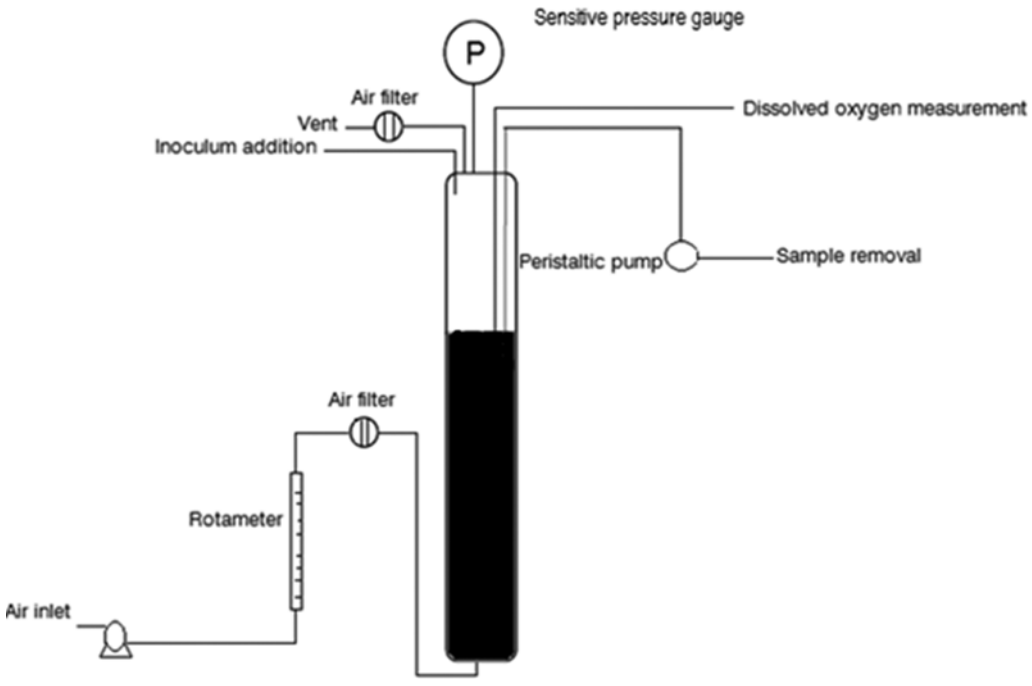

Fig. 1. Schematic of the experimental set-up.

ment [23], ultrasonication [24,25], emulsification [26,27] and supercritical extraction [28,29].

In the present study, one variable-at-a-time (OVAT) experimental data was first used to obtain an empirical model using an artificial neural network correlating air flow rate, inoculum size and incubation time, which was then optimized using genetic algorithm to calculate the optimal operating conditions for zeaxanthin production by *Paracoccus zeaxanthinifaciens* ATCC 21588 in a bubble column bioreactor. The effect of ANN-GA optimization on power consumed per unit volume (P/V_L) and energy input (E), was further studied. To the best of our knowledge, this is the first-ever report on OVAT results based ANN-GA optimization of any microbial metabolite production in a bubble column reactor and analysis of the engineering parameters involved.

MATERIALS AND METHODS

1. Chemicals

All the chemicals used in the present study were of analytical grade unless otherwise stated. Zeaxanthin used as the standard pigment was obtained as a gift from OmniActive Health Technologies Ltd., Mumbai.

2. Microorganism and Culture Conditions

The microorganism used in this work, *Paracoccus zeaxanthinifaciens* ATCC 21588, was obtained from BCCM/LMG, Ghent University, Belgium. The culture was maintained in yeast-tryptone-sodium slants at 4 °C [30]. Seed cultures were obtained by inoculating two loop full of culture from a 48 h old slant into 80 mL production medium in 500 mL Erlenmeyer flasks followed by incubation at 30 °C for 24 h with agitation (180 rpm). The bubble column reactor was inoculated with 40 and 80 mL of the above prepared seed culture according to process requirements.

3. Fermentation Conditions

Fermentation was in a 1.5 L bubble column reactor (Height-55 cm; diameter-6 cm) made of glass with a working volume of 1 L (Fig. 1). The ANN-GA optimized buffered production medium containing glucose (2.4%), yeast extract (3%), sodium chloride (0.8%), magnesium sulfate (0.5%), methyl palmitate (0.8%), malic acid (30 mM), ferrous sulfate (10 mM) and pyridoxine hydrochloride (0.18 mg/L) was used for *Paracoccus zeaxanthinifaciens* ATCC 21588 cultivation in the bioreactor [31]. The reactor was incubated at 30 °C in a controlled temperature chamber, and sterile air was supplied through a stainless steel ring sparger provided at the bottom of the column with an air pump at different flow rates (2-5 L/min) using a precalibrated rotameter. Dissolved oxygen concentration in the fermentation broth was measured with a dissolved oxygen probe (HI 768040, Hanna Instruments, USA) [32]. To account for loss of water from the medium due to entrainment at high specific air flow rate, sterilized distilled water was added into the medium with a peristaltic pump [11]. Foaming encountered during the fermentation period was controlled by dropwise addition of sterile silicone based antifoam.

4. Analytical Methods

Samples were aseptically withdrawn from the bubble column reactor after every 10 h and centrifuged (8,000 g for 20 min) at 4 °C. The cell pellet obtained was repeatedly washed with normal saline, centrifuged and subsequently lyophilized. As there are reports on partial extracellular secretion of carotenoids by bacteria of the genus *Paracoccus* [33,34], both lyophilized biomass and cell-free supernatant were analyzed for the presence of zeaxanthin as described by Joshi and Singhal [31]. In brief, zeaxanthin from the cells was recovered by subjecting the lyophilized cell mass (0.1 g) to ultrasonication at 20 kHz in 10 mL tetrahydrofuran containing 0.01% (w/v) butylated hydroxy toluene for 10 min while zeaxan-

thin secreted into the production medium was recovered by extracting the supernatant twice with equal volumes of 2-methyl tetrahydrofuran containing 0.01% (w/v) butylated hydroxy toluene at 60 °C. The fractions containing extracted zeaxanthin were then evaporated to complete dryness using a rotary evaporator, redissolved in known volume of tetrahydrofuran and pooled together to obtain the zeaxanthin produced.

Zeaxanthin concentration was quantitatively analyzed by high-performance thin layer chromatography (HPTLC) [31,35]. HPTLC was performed on silica gel 60 HPTLC plates (E. Merck, Mumbai) using an HPTLC system (CAMAG, Switzerland) equipped with an automated Linomat-V applicator and winCATS (version 1.4.3.6336) controlled TLC scanner III. The mobile phase consisted of chloroform/ethanol/butylated hydroxy toluene (95 : 5 : 0.01 v/v/w). After development and drying, quantitative densitometry of the zeaxanthin band (R_f=0.52) was carried out at 470 nm with a slit dimension of 6.0 mm×0.45 mm and a scanning speed of 20 mm/s using a deuterium lamp [31]. Zeaxanthin concentration was calculated by interpolation from a zeaxanthin standard curve established under similar conditions. Quantification was performed in dim light to avoid photodegradation.

For biomass determination, 2 mL of the fermentation broth was centrifuged in preweighed Eppendorf tubes followed by repeated washing and finally drying at 60 °C for 24 h. GOD-POD test kit was used to determine glucose in the medium during fermentation [36].

All the experiments were carried out in triplicates and the data presented are the mean values±SD. Statistical analysis of the data was performed by employing student's t test ($P<0.05$) using Microsoft Excel.

5. Power Consumption Per Unit Liquid Volume and Energy Input Calculation

The power input per unit liquid volume was obtained by applying a macroscopic energy balance on a unit mass basis for the gas

Table 1. Effects of varying air flow rate (Q) and inoculum size (I) on experimental zeaxanthin production for different incubation time (t) along with corresponding power consumed per unit volume (P/V_L), energy consumption (E) and ANN predicted zeaxanthin production

Run	Air flow rate, Q (vvm)	Inoculum size, I (% v/v)	Incubation time, t (h)	Power input per unit liquid volume, P/V_L (W/m^3)	Energy input, E (kJ)	Zeaxanthin, Z (mg/L)	
						Experimental	Predicted
1	2	4	30	118.56	12.80	6.67±0.37	6.68
2	2	4	40	118.78	17.10	7.88±0.29	7.86
3	2	4	50	115.22	20.74	11.22±0.43	11.22
4	2	4	60	115.33	24.91	11.57±0.46	11.51
5	2	4	70	112.09	28.25	8.47±0.22	8.49
6	2	4	80	111.99	32.25	8.13±0.03	8.11
7	3	4	30	168.24	18.17	7.88±0.31	7.86
8	3	4	40	173.27	25.70	9.15±0.54	9.16
9	3	4	50	173.11	31.19	12.21±0.18	12.21
10	3	4	60	168.08	37.39	12.96±0.26	12.94
11	3	4	70	168.40	42.36	11.13±0.59	10.62
12	3	4	80	175.57	48.50	10.57±0.28	10.58
13	4	4	30	238.08	25.71	9.31±0.55	9.32
14	4	4	40	238.53	34.35	11.32±0.34	10.72
15	4	4	50	231.35	41.64	13.22±0.22	13.20
16	4	4	60	231.57	50.02	13.76±0.14	13.77
17	4	4	70	224.62	56.60	11.70±0.40	11.79
18	4	4	80	224.83	64.75	11.24±0.11	11.53
19	5	4	30	297.99	32.18	7.19±0.38	8.37
20	5	4	40	298.55	43.00	9.27±0.25	9.23
21	5	4	50	289.56	52.12	11.04±0.33	11.04
22	5	4	60	289.56	62.54	11.21±0.21	11.81
23	5	4	70	281.65	70.98	8.69±0.08	8.73
24	5	4	80	281.39	81.04	8.11±0.48	8.19
25	4	8	30	239.30	25.84	7.61±0.41	7.60
26	4	8	40	238.85	34.39	8.14±0.46	8.65
27	4	8	50	232.54	41.86	9.46±0.63	9.67
28	4	8	60	232.32	50.18	10.22±0.20	9.72
29	4	8	70	225.35	56.79	9.39±0.16	9.44
30	4	8	80	224.72	64.72	8.44±0.39	8.31

phase [37] as shown below:

$$\Delta\left(\frac{1}{2}u^2\right)+\Delta\Phi+\int_{P_o}^{P_{sf}}\frac{dP}{\rho_g}+\overline{W}+\overline{E_v}=0 \quad (1)$$

where u is the gas velocity, $\Delta\Phi$ is change in potential energy, $\overline{E_v}$ is the frictional loss, $\overline{W}$ is the work done, P_o and P_{sf} are the pressure values above the sparger and the liquid surface, respectively.

Neglecting the values of $\Delta\Phi$ and $\overline{E_v}$, the work done by unit mass of gas can be represented as:

$$\overline{W}=\frac{RT}{M}\ln\frac{P_o}{P_{sf}}+\frac{\eta u_o^2}{2} \quad (2)$$

where R is the molar gas constant, T is the absolute temperature and M is the molar mass of gas.

Since the production medium was assumed to behave like dilute solutions, on further neglecting η due to its lower value and solving Eq. (2), the following expression for power input (P) per unit liquid volume (V_L) was obtained:

$$\frac{P}{V_L}=\frac{Q_M}{V_L}\rho_L gH \quad (3)$$

where $Q_M=Q(P_{sf}/P_{LM})$, $P_{LM}=((P_o-P_{sf})/\ln(P_o/P_{sf}))$, ρ_L is the liquid density, g is the acceleration due to gravity, Q is the air flow rate and H is the height of the liquid column.

The energy consumption by the aerator during the fermentation process was then calculated using the following relationship:

$$E=Q_M\rho_L gH\times t \quad (4)$$

where t is the incubation time

6. Sequential One-variable-at-a-time Approach

To determine optimal combination of inputs for maximum zeaxanthin production, the effects of varying air flow rate (2-5 vvm) and inoculum size (4 and 8%; cell count - 5.3×10^8 cells/mL) for different time of incubation (30-80 h) were evaluated sequentially using traditional OVAT methodology (Table 1).

7. Artificial Neural Network

A feed-forward ANN with back propagation training algorithm was developed to model zeaxanthin production by *Paracoccus zeaxanthinifaciens* ATCC 21588 in the bubble column reactor. For ANN-based empirical model development, the OVAT input-output data was randomly apportioned into three sets: training (70%), validation (15%) and testing (15%). A feedforward back propagation neural network with three neurons, air flow rate (Q), inoculum size (I) and incubation time (t) as inputs in the input layer, and six hidden neurons (N1-N6, one hidden layer with hyperbolic sigmoid transfer function, *tansig*) with one output in the output layer (with linear transfer function, *purelin*), zeaxanthin production (Z), was then created in Matlab 2013b (Mathworks, Natick, USA). The Levenberg-Marquardt back propagation algorithm (*trainlm*), which is known to be the most agile training algorithm, was used for network training [26]. The transfer functions, *purelin* and *tansig* are defined as

$$\text{purelin}(x)=x \quad (5)$$

$$\tan\text{sig}(x)=\frac{1-\exp(-x)}{1+\exp(-x)} \quad (6)$$

Fig. 2 shows the ANN architecture used in this study. A single hidden layer was chosen as it can interpret majority of input-output structure with high efficiency when provided with optimum number of hidden neurons. Moreover, the optimum number of hidden neurons (six in the present study) was determined by mean square error (MSE) analysis performed by varying the number of hidden neurons from 2-10 [24].

8. Genetic Algorithm

GA is an iterative, population-based optimization algorithm that attempts to solve complex problems by mimicking the process of natural selection using various genetic operators like selection, crossover and mutation. The GA-based optimization parameters were chosen as reported in literature [26] and are listed in Table 2. The optimization was executed by using the optimally trained nonlinear ANN model as the fitness function with following lower and upper bound values of the process input parameters (air flow rate, inoculum size and incubation time) used in the OVAT experiments:

$$\begin{cases} 2\le Q\le 5 \\ 4\le I\le 8 \\ 30\le t\le 80 \end{cases}$$

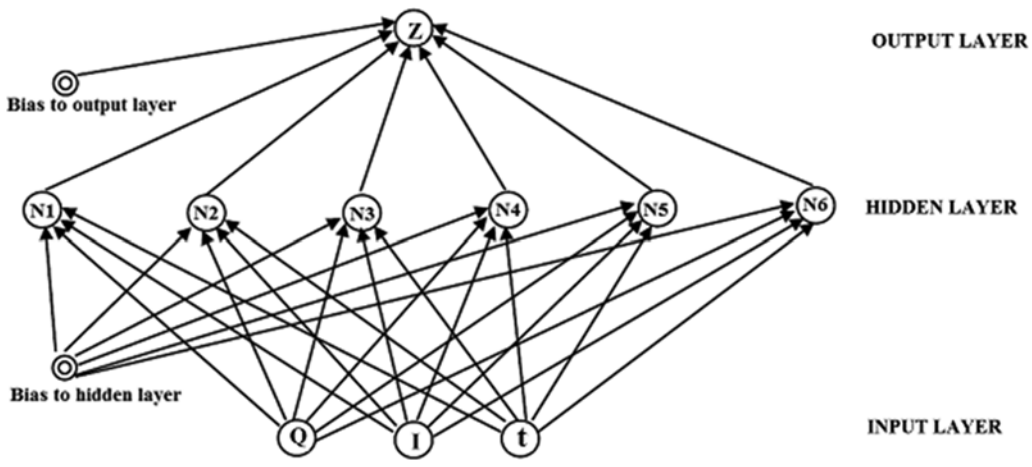

Fig. 2. Pattern of ANN architecture used in the present study.

Table 2. GA criterion leading to an optimal solution

Parameters	Function types/values
Population size	50
Scaling function	Rank
Selection function	Roulette wheel
Crossover function	Heuristic
Crossover rate	0.8
Mutation function	Adaptive feasible
Direction of migration	Forward
Migration fraction	0.2
Generation	100

RESULTS AND DISCUSSION

1. Optimization by One-variable-at-a-time Approach

The purpose of these experiments was to determine the optimum combination of air flow rate (Q, vvm), inoculum size (I, % v/v) and incubation time (t, h) which would result in maximum zeaxanthin production. The effects of the aeration rate and inoculum size on zeaxanthin concentration and biomass production are shown in Fig. 3(a)-(b). In all the different combinations studied, zeaxanthin was found to be produced in two phases: In the first phase (0 to 30 h of incubation) called "logarithmic phase," and in the second step (30 to 80 h of incubation) called "stationary phase" (Fig. 3(a) and 3(b)). Zeaxanthin production during the logarithmic phase can be attributed to high respiratory activity of the actively growing cells, which results in the production of large quantities of reactive oxygen species, which in turn stimulates zeaxanthin production [38]. Zeaxanthin production and secretion into the production medium by *Paracoccus zeaxanthinifaciens* ATCC 21588 during the stationary phase could be attributed to the presence of indigenous multidrug transporters and different ATP-binding cassette transporters present in the bacterial cells. These transporters have been reported to play an important role in secretion of carotenoids outside the cells [39,40]. Carotenoids secretion during the stationary phase by *Paracoccus marcusii* has earlier been reported by Hirschberg and Harker [34].

Zeaxanthin concentration increased significantly at constant inoculum size of 4% (v/v) as the air flow rate was increased from 2 vvm to 4 vvm. However, a further increase of the air flow rate over 4 vvm resulted in a decrease in zeaxanthin concentration (Fig. 3(a)). Highest concentration of zeaxanthin (13.76±0.14 mg/L) was obtained at an air flow rate of 4 vvm after 60 h of incubation and decreased sharply thereafter (Table 1). Similar sharp reduction in zeaxanthin concentration after optimum incubation time has been reported in shake flask experiments involving *Maricauda* sp. [41]. The decline in zeaxanthin concentration after 60 h could possibly be due to degradation of the pigment by the action of oxidative enzymes present in the bacterial cells. Further, with increase in inoculum size from 4% to 8% at a constant air flow rate of 4 vvm, the biomass production increased slightly from 9.78±0.31 g/L to 10.45±0.17 g/L, but zeaxanthin production decreased significantly from 13.76±0.14 mg/L to 10.22±0.20 mg/L after optimum incubation time of 60 h (Fig. 3(a) and 3(b)).This highly significant decrease in zeaxanthin production could possibly be due to shortage of available nutrients at large inoculum size [42].

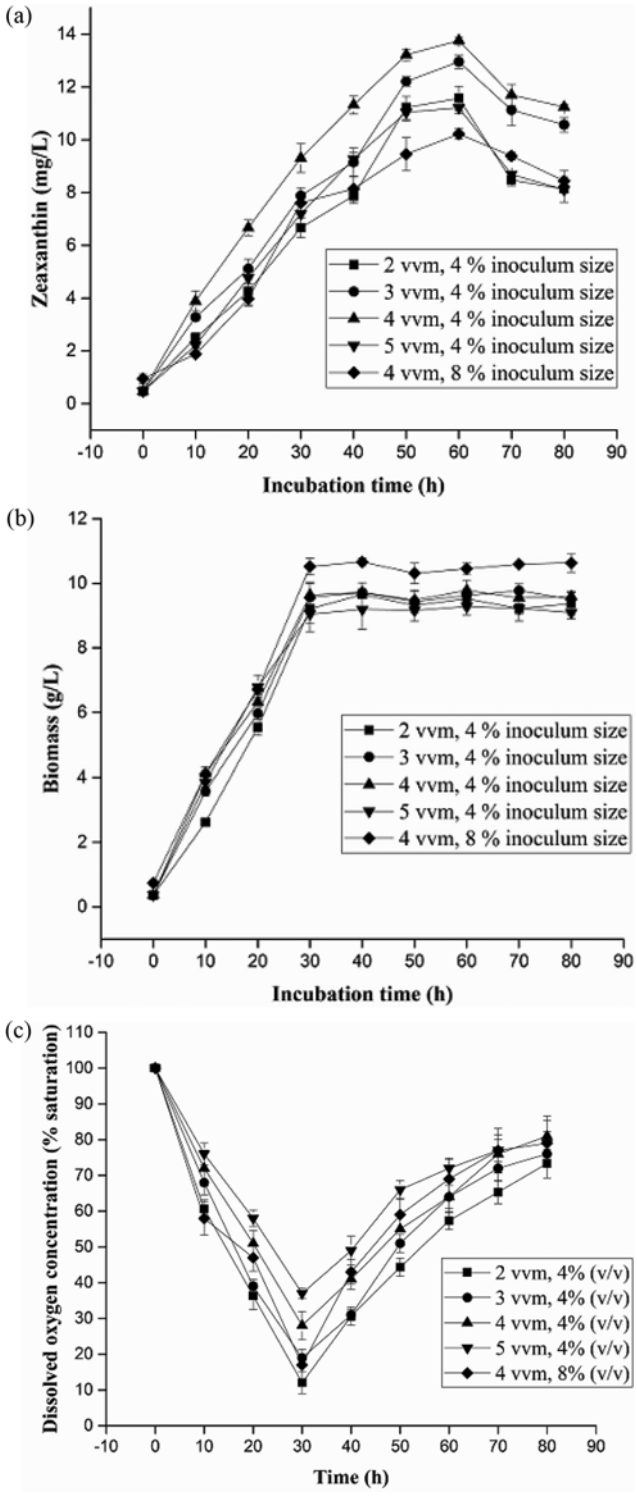

Fig. 3. Effect of the aeration and inoculum size on (a) zeaxanthin production (b) biomass production (c) dissolved oxygen concentration during the course of fermentation.

In all the different aeration-inoculum size combination studied, the dissolved oxygen concentration decreased rapidly during 0-30 h of incubation and then increased until the end of the fermen-

tation (Fig. 3(c)). This rapid decrease was probably due to the rapid increase in biomass concentration observed during the logarithmic phase (Fig. 3(b)). An increase in the dissolved oxygen concentration after 30 h of incubation, on the other hand, was due to the constant biomass concentration observed at the stationary phase (Fig. 3(b)). In the cultures grown at aeration rates of 2, 3, 4 and 5 vvm using an inoculum size of 4% (v/v), the minimum and maximum dissolved oxygen concentration was 12%, 19%, 28%, 39% and 71%, 76%, 81% and 79%, respectively (Fig. 3(c)). On the other hand, with an aeration-inoculum size combination of 4 vvm - 8% (v/v) the minimum and maximum dissolved oxygen concentration was 17% and 79%, respectively. A similar trend for dissolved oxygen concentration was earlier reported by Nanou et al. [11] for carotene production by *Blakeslea trispora* in a bubble column reactor.

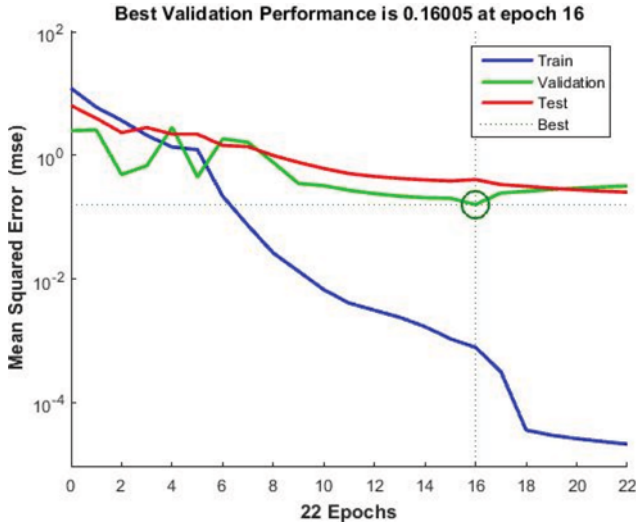

Fig. 4. Performance plot of the ANN model (3-6-1) in the training phase showing performance value (MSE- 0.16005) after 16 epochs.

2. Process Modeling Using Artificial Neural Network

Neural network training, testing and validation were performed with 20, 5 and 5 data sets of the OVAT experiments, respectively. Initially, the weights were selected at random and later an iterative

Table 3. Mean square error and correlation values for the developed ANN model

Process	Samples	Mean square error (MSE)	Correlation (R)
Training	20	7.82e-4	0.999
Validation	5	1.60e-1	0.959
Testing	5	4.04e-1	0.942
All	30	9.46e-2	0.987

Table 4. Weight and bias values of nonlinear ANN model

Neuron no.	Weights from input layer to hidden layer			Bias to hidden layer	Weights from hidden layer to output layer	Bias to output layer
	Air flow rate	Inoculum	Time			
1	−1.186	−0.416	2.249	2.079	−0.386	1.247
2	0.214	0.821	−3.800	1.591	−0.907	
3	4.465	0.289	0.364	1.824	−0.508	
4	0.293	1.032	−3.072	0.562	1.016	
5	4.292	1.279	1.381	−3.166	0.532	
6	−1.680	1.586	−2.587	−2.419	0.122	

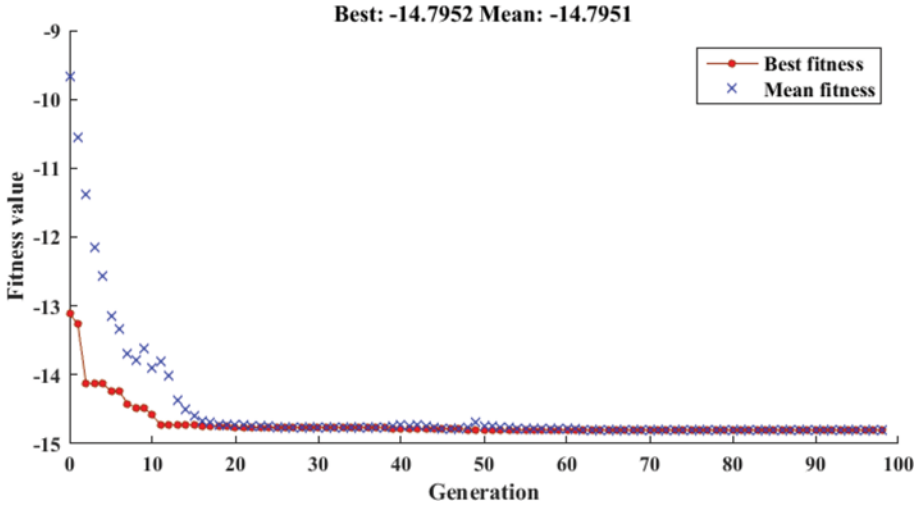

Fig. 5. ANN-GA model simulated fitness function plot. Best and average fitness values show a gradual convergence towards the optimum value of 14.79 after 98 generations.

Table 5. Comparative results of confirmatory experiments for model validation

Optimization approach	Process input parameters			Zeaxanthin (mg/L)	Volumetric power input, P/V_L (W/m^3)	Energy consumed, E (kJ)
	Q (vvm)	I (% v/v)	t (h)			
OVAT	4	4	60	13.76±0.14	231.57	50.02
ANN-GA (predicted)	3.507	4	55.81	14.79	-	-
ANN-GA (experimental)	3.5	4	55	15.09±0.51	202.03	40.01

algorithm was used to find their values that minimized the differences between the actual OVAT outputs and network-calculated outputs. The ANN training was performed for 100 epochs after which the lowest MSE value of 0.160 for the validation data set was observed and the network stopped training (Fig. 4). Network's performance was assessed using mean squared error (MSE) and regression analysis [20]. The correlation values (R) of 0.999, 0.942 and 0.959 for training, testing and validation data sets, respectively, confirmed the efficacy of the developed neural network model (Table 3). Table 4 shows the values of weights and bias for the optimally trained neural network.

3. Optimization Using Genetic Algorithm and Model Validation

Once trained, the trained neural network served as fitness function for the genetic algorithm (GA). Zeaxanthin production predicted by ANN-GA after 98 generations (Fig. 5) was 14.79 mg/L at 3.507 vvm of air flow rate and 4% inoculum size after 55.81 h of incubation. Laboratory validation at bioreactor operational conditions of 3.5 vvm and 4% inoculum after 55 h of incubation (Table 5) resulted in a zeaxanthin concentration of 15.09±0.51 mg/L, which is significantly close to the GA predicted production. During the validation run, zeaxanthin production was monitored up to 80 h at regular intervals and correlated with the biomass growth and glucose consumption (Fig. 6(a)).

Under ANN-GA determined operational combination, a rapid increase in biomass was observed during the logarithmic phase (0 to 30 h of incubation) of the bacterial growth (Fig. 6(a)). With increase in biomass, the oxygen demand of the culture also increased and hence, a sharp decrease in dissolved oxygen concentration of the broth was observed (Fig. 6(b)). After 30 h of incubation, no significant change in biomass concentration of the broth was observed and the culture entered the stationary phase (30 to 80 h of incubation) of growth. During this period, the dissolved oxygen concentration again started increasing as shown in Fig. 6(b). The minimum and maximum dissolved oxygen concentrations obtained during the entire fermentation batch run were 24% and 77%, respectively (Fig. 6(b)).

Zeaxanthin production increased with the time of incubation during the logarithmic phase with a maximum production of 8.37±0.39 mg/L achieved after 30 h of incubation (Fig. 6(a)). Zeaxanthin secretion outside the cells was, however, observed only during the stationary phase and a maximum concentration of 6.69±0.18 mg/L was recovered from the fermentation broth after 55 h of incubation. It was observed that up to 55 h of incubation during the stationary phase (30 to 55 h), the culture was able to successfully replenish the amount of zeaxanthin secreted outside the cells and, thus, no significant change in intracellular zeaxanthin concentration was observed. Similar observation on replenishment of the levels of intracellular carotenoids was earlier reported in the case of heterologous carotenoids production by *Escherichia coli* [40]. Beyond 55 h of incubation at optimized condition, a significant decrease in zeaxanthin production was observed (Fig. 6(a)), which probably was due to oxidative enzymes based degradation of zeaxanthin [9,11].

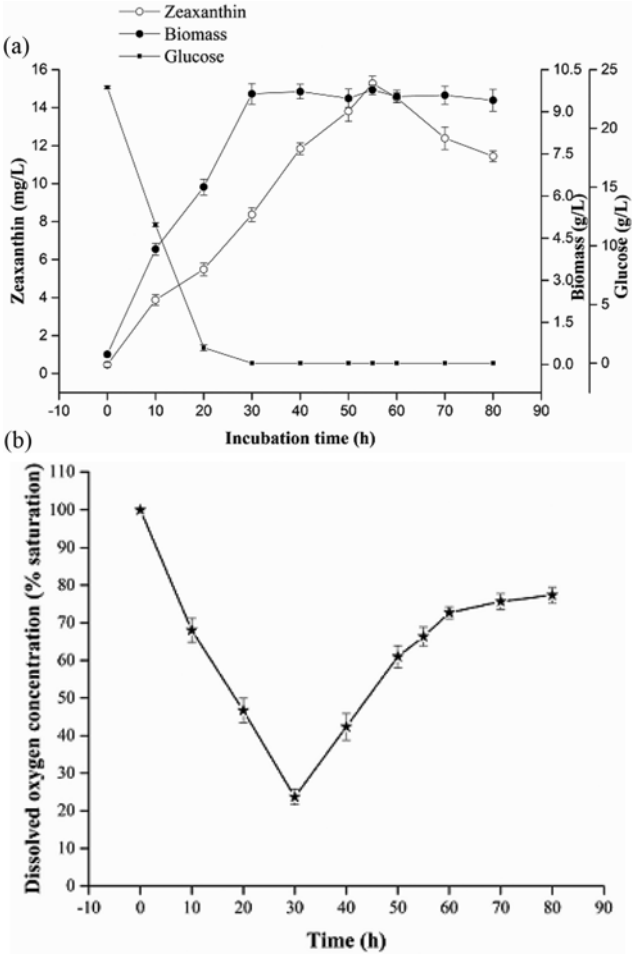

Fig. 6. Fermentation kinetics at ANN-GA optimized conditions (a) zeaxanthin production with respect to dry biomass and glucose concentration during the due course of fermentation for 80 h (b) dissolved oxygen concentration profiling.

Hirschberg and Harker [34] earlier reported excretion of carotenoids by *Paracoccus marcusii* during the stationary phase in which the secreted carotenoids accounted to as much as 80% of the total carotenoids produced. Joshi and Singhal [31] recently reported a

maximum zeaxanthin production of 11.63 mg/L by *Paracoccus zeaxanthinifaciens* 21588 in shake flask experiments with approximately 36% (4.14 mg/L) of it being recovered from the cell free fermentation broth. It can be seen that zeaxanthin production by *Paracoccus zeaxanthinifaciens* 21588 significantly enhanced when the process was scale transformed from shake flask level to reactor scale. This was probably due to superior dissolved oxygen profile, better mixing regime and elevated levels of oxidative stress obtained in the bubble column reactor under optimized operational combination [10,11].

4. Analysis of Volumetric Power Input (P/V_L) and Energy Requirements for GA-based Fermentation Model

The mean volumetric power input to the bubble column at constant inoculum size of 4% (v/v) increased linearly at the rate of 115.33±2.97 W/m^3 for 2 vvm, 171.11±3.27 W/m^3 for 3 vvm, 231.50 ±6.08 W/m^3 for 4 vvm, and 289.78±7.50 W/m^3 for 5 vvm during the due course of incubation (30-80 h) (Table 1). An optimal zeaxanthin production of 13.76±0.14 mg/L using an aeration-inoculum size combination of 4 vvm - 4% (v/v) in OVAT experiments was achieved at the expense of 231.57 W/m^3 of volumetric power input corresponding to an energy input of 50.02 kJ drawn by the aerator (Table 1). The ANN-GA approach, on the other hand, led to only a slight increase (9.7%) in zeaxanthin production, although at an expense of 202.03 W/m^3 of volumetric power input corresponding to an energy input of 40.01 kJ (Table 2). Thus, the ANN-GA predicted optimum was better both in terms of metabolite production and energy input to the bubble column.

CONCLUSIONS

Agitation, incubation time and inoculum size are the most important parameters for process optimization in submerged aerobic fermentations in bubble column reactors. The optimal mode of bioreactor operations for fermentative production of zeaxanthin was developed using GA-based optimization model and compared with traditional OVAT method. GA-simulated optimization model enabled zeaxanthin production to increase by 9.7% along with 20% reduction in the energy input. The proposed OVAT based ANN-GA optimization approach can thus be used to determine an optimum and energy efficient operational combination on a pilot/commercial scale.

ACKNOWLEDGEMENTS

The project was financially assisted by UGC-SAP, New Delhi, India. Authors are also grateful to Mr. Sreekanth MS from IIT, Mumbai for his generous help with Matlab for neural network and genetic algorithm simulations.

ETHICAL APPROVAL

This article does not contain any studies with human participants or animals.

REFERENCES

1. J. D. Ribaya-Mercado and J. B. Blumberg, *J. Am. Coll. Nutr.*, **23**, 567S (2004).
2. E. Loane, J. M. Nolan, O. O'Donovan, P. Bhosale, P. S. Bernstein and S. Beatty, *Surv. Ophthalmol.*, **53**, 68 (2008).
3. R. L. Roberts, J. Green and B. Lewis, *Clin. Dermatol.*, **27**, 195 (2009).
4. S. M. Moeller, P. F. Jacques and J. B. Blumberg, *J. Am. Coll. Nutr.*, **19**, 522S (2000).
5. P. Thawornwiriyanun, S. Tanasupawat, C. Dechsakulwatana, S. Techkarnjanaruk and W. Suntornsuk, *Appl. Biochem. Biotechnol.*, **167**, 2357 (2012).
6. M. Y. Victor and S. K. Bhatia, *Biotechnol. Lett.*, **34**, 1405 (2012).
7. Y. T. Cheng and C. F. Yang, *J. Taiwan Inst. Chem. Eng.*, **61**, 270 (2016).
8. A. Berry, D. Janssens, M. Hümbelin, J. P. Jore, B. Hoste, I. Cleenwerck, M. Vancanneyt, W. Bretzel, A. F. Mayer, R. Lopez-Ulibarri and B. Shanmugam, *Int. J. Syst. Evol. Microbiol.*, **53**, 231 (2003).
9. A. J. Schocher and O. Wiss, US Patent, 3,891,504 (1975).
10. P. M. Doran, *Bioprocess engineering principles*, Academic Press, London (1995).
11. K. Nanou, T. Roukas and E. Papadakis, *Biochem. Eng. J.*, **54**, 172 (2011).
12. K. Nanou, T. Roukas and E. Papadakis, *Biochem. Eng. J.*, **67**, 203 (2012).
13. P. F. Stanbury, A. Whitaker and S. J. Hall, *Principles of fermentation technology*, Elsevier (2013).
14. L. M. Hao, L. Z. Xing, J. C. Zhang, J. X. Sun, S. R. Jia, C. S. Qiao and T. Wu, *Appl. Biochem. Biotechnol.*, **160**, 621 (2010).
15. D. Dursun and A. C. Dalgıç, *Biocatal. Agric. Biotechnol.*, **7**, 1 (2016).
16. E. B. Eryılmaz, D. Dursun and A. C. Dalgıç, *Biocatal. Agric. Biotechnol.*, **7**, 224 (2016).
17. K. R. Pandey, C. Joshi and B. V. Vakil, *SpringerPlus*, **5**, 1654 (2016).
18. C. H. Kuo, T. A. Liu, J. H. Chen, C. M. J. Chang and C. J. Shieh, *Biocatal. Agric. Biotechnol.*, **3**, 1 (2014).
19. A. A. Babaei, A. Khataee, E. Ahmadpour, M. Sheydaei, B. Kakavandi and Z. Alaee, *Korean J. Chem. Eng.*, **33**, 1352 (2016).
20. D. Singh and G. Kaur, *Bioproc. Biosyst. Eng.*, **37**, 1599 (2014).
21. M. Zafar, S. Kumar and A. K. Dhiman, *Biocatal. Agric. Biotechnol.*, **1**, 70 (2012).
22. A. A. Prabhu, B. Mandal and V. V. Dasu, *Korean J. Chem. Eng.*, **34**, 1109 (2017).
23. P. Kundu and I. M. Mishra, *Desalination Water Treat.*, **57**, 19713 (2016).
24. S. M. Huang, C. H. Kuo, C. A. Chen, Y. C. Liu and C. J. Shieh, *Ultrason. Sonochem.*, **36**, 112 (2017).
25. Z. İlbay, S. Şahin and K. Büyükkabasakal, *Korean J. Chem. Eng.*, **31**, 1661 (2014).
26. P. Kundu, V. Paul, V. Kumar and I. M. Mishra, *Chem. Eng. Res. Des.*, **104**, 773 (2015).
27. P. Kundu, V. Paul, V. Kumar and I. M. Mishra, *Petrol. Sci. Technol.*, **34**, 350 (2016).
28. E. M. E. M. Shokir, E. S. Al-Homadhi, O. Al-Mahdy and A. A. H. El-Midany, *Korean J. Chem. Eng.*, **31**, 1496 (2014).
29. P. Davoodi, S. M. Ghoreishi and A. Hedayati, *Korean J. Chem. Eng.*, **34**, 854 (2017).
30. M. G. Sajilata, M. V. Bule, P. Chavan, R. S. Singhal and M. Y. Kamat, *Sep. Purif. Technol.*, **71**, 173 (2010).

31. C. Joshi and R. S. Singhal, *Biocatal. Agric. Biotechnol.*, **8**, 228 (2016).
32. D. S. Savić, M. L. Lazić, V. B. Veljković and M. M. Vrvić, *Chem. Ind. Chem. Eng.*, **11**, 59 (2005).
33. K. Hirasawa and A. Tsubokura, U.S. Patent, 8,853,460 (2014).
34. J. Hirschberg and M. Harker, U.S. Patent, 5,935,808 (1999).
35. S. Rosa-Putra, A. Hemmerlin, J. Epperson, T. J. Bach, L. H. Guerra and M. Rohmer, *FEMS Microbiol. Lett.*, **204**, 347 (2001).
36. V. Ferreira, M. D. O. Faber, S. D. S. Mesquita and N. Pereira Jr., *Electron. J. Biotechnol.*, **13**, 5 (2010).
37. D. S. Clark and H. W. Blanch, *Biochemical Engineering*, CRC Press (1997).
38. P. Bhosale, A. J. Larson and P. S. Bernstein, *J. Appl. Microbiol.*, **96**, 623 (2004).
39. R. Verwaal, Y. Jiang, J. Wang, J. M. Daran, G. Sandmann, J. A. van den Berg and A. J. van Ooyen, *Yeast*, **27**, 983 (2010).
40. R. Doshi, T. Nguyen and G. Chang, *PNAS*, **110**, 7642 (2013).
41. S. Prabhu, P. D. Rekha, C. C. Young, A. Hameed, S. Y. Lin and A. B. Arun, *Appl. Biochem. Biotechnol.*, **171**, 817 (2013).
42. C. Sandhya, A. Sumantha, G. Szakacs and A. Pandey, *Process Biochem.*, **40**, 2689 (2005).